Transmission of 18 keV negative ions Cl^- through nanocapillariesin Al_2O_3 membrane*

Lü Xue-Yang(吕学阳), Chen Lin(陈 林), Chen Xi-Meng(陈熙萌)†, Jia Juan-Juan(贾娟娟), Zhou Peng(周 鹏), Zhou Chun-Lin(周春林), Qiu Xi-Yu(邱玺玉), Shao Jian-Xiong(邵剑雄), Cui Ying(崔 莹), Yin Yong-Zhi(尹永智), Wang Hong-Wei(王宏伟), and Ji Ming-Chao(姬明超)

School of Nuclear Science and Technology, Lanzhou University, Lanzhou 730000, *China*

(Received 12 January 2010; revised manuscript received 3 June 2010)

We investigate the angular distribution of the transmitted 18keV negative ions Cl^- through Al_2O_3 nanocapillaries of 50 nm in diameter and 10 μm in length. Elastic scattering ions and inelastic scattering ions are obtained simultaneously. The experimental result is partially consistent with the guiding effect. We can qualitatively explain our experimental result through a dynamic process.

Keywords: nanocapillaries, negative ions, angular distribution, guiding effect

PACS: 34.50.–s, 34.50.Gb, 37.20.+j **DOI:** 10.1088/1674-1056/20/1/013401

Advances in the field of nanostructures in recent years made it possible to manufacture membrane with straight and large aspect ratio nanosized capillaries in various materials. Subsequently, one has paid paticular attention to properties of the nanocapillaries of high aspect ratio. A tool to characterize the electric properties of capillaries is slow highly charged ions. Originally, the extraction of substrate hollow atom was studied by Yamazaki[1] and Ninomiya *et al.*[2] with capillaries in conducting metallic materials, whose surface properties were well known. Measurements by Stolterfoht *et al.*[3−6] showed that in contrast to metallic capillary arrays, there existed guiding phenomenon of slow highly charged ions (HCIs) passing through a membrane of capillaries in insulating polyethylene terephthalate (PET) even when the membrane was tilted a few degrees so that it was not geometrically transparent to the ion beam. Recently, there has been much research devoted to different capillary materials, such as PET, PC, SiO_2 and Al_2O_3.[7−10] The results of these measurements also show that large majority of transmitted ions retain their initial charge states and kinetic energies, with exit angle close to the title angle.

The major explanation of the guiding phenomenon was given by Stolterfoht *et al.*[3−6] and Hellhammer *et al.*[11,12] They believed that incident ions deposited charges near the inner wall of the capillaries in a self-organizing pattern that prevented these charges from closely contacting the inner wall. Recently Monte Carlo simulations showed that entrance charge patch was the main deflection point and possibly a second weaker patch further inside the capillaries was more and more prevalent.[13−15] The investigation of the guiding effect deviated far from the use of HCIs and electrons as projectiles before 2008, but guiding effect was found. Negative ions can also play a very important role in many fields such as plasma, atmosphere, laser and chemistry. In 2009 the experiment on negative ions(O^-) impact of nanocapillaries was conducted by our group.[16]

In the present work, the negative ions are used to impact Al_2O_3 membrane with capillaries of 50 nm in diameter and 10 μm in length. The work is focused on the angular distribution of the transmitted ions. The experiment was performed at the Laboratory of Tandem Electrostatic Accelerator of Lanzhou University. The set-up of experiment was described in Fig. 1. The insulating membrane was mounted on a goniometer in the centre of a chamber allowing independent adjustment in two axial dimensions and around one rotational axe. The ions were extracted from a sputtering ion source and selected by an analysis magnet. Two 1.5×2 mm apertures with 35 mm spacing between the magnet and target were used to collimate the beam. A parallel-plate electrostatic analyzer was set to analyse charge state distributions of the transmitted ions. The transmitted ions were detected by one-dimensional position-sensitive microchannel plate (1D-PSMCP) detector. The chamber and the beam line were operated with a base pressure of 2.5×10^{-5} Pa.

*Project supported by the National Natural Science Foundation of China (Grant No. 10775063).

†Corresponding author. E-mail: chenxm@lzu.edu.cn

© 2011 Chinese Physical Society and IOP Publishing Ltd

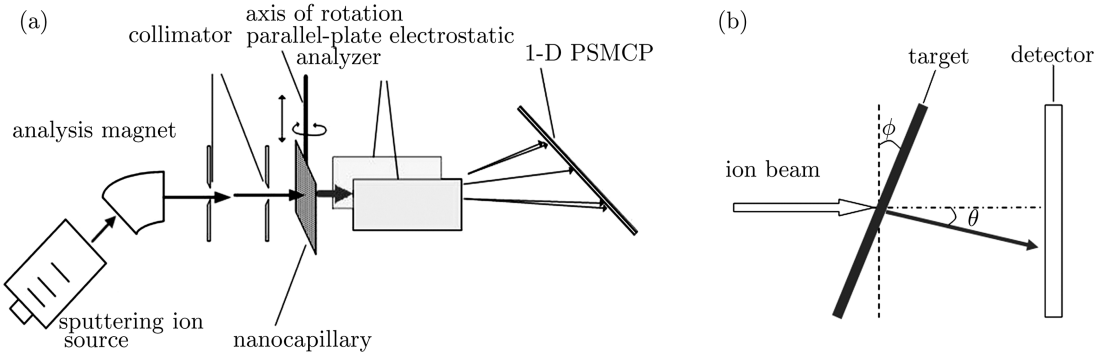
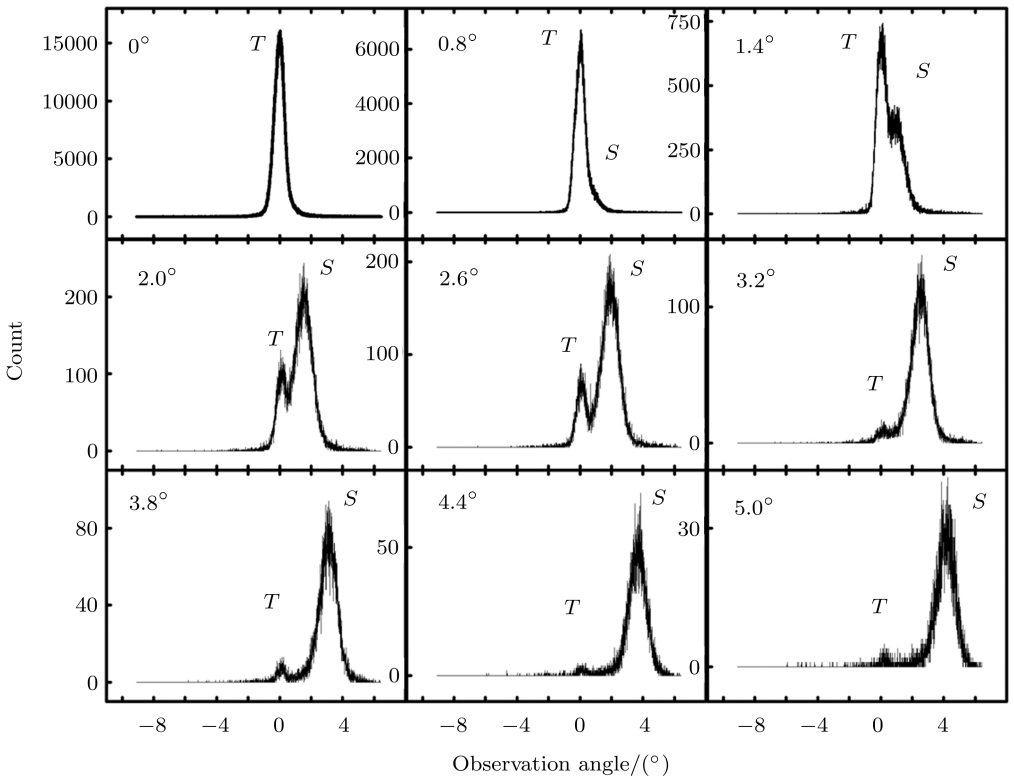


Fig. 1. Diagrams of ion beam (a) and angle setting (b). Panel (a) shows the ions extracted from the sputtering ion source and selected by an analysis magnet, two 1.5×2 mm apertures with 35 mm spacing between the magnet and target for collimating the beam and transmitted ions detected by one-dimensional position-sensitive micro-channel plate (1D-PSMCP) detector. Panel (b) indicates the meanings of tilt angle ϕ and observation angle.

In this paper, we present our experimental result, i.e., the angular profile of the transmitted ions as a function of ionic energy, and we try to use a dynamic process to explain the phenomenon.

Figure 2 shows the angular distributions each as a function of observation angle for different values of capillary tilt angle ϕ, but they are different from those in the previous work: in Fig. 2 there appear two prominent peaks labeled as T and S. Peak T is nearly in the direction of the ion beam. Another peak was labeled as S ions, implying that the ions are scattered from the inner wall of the capillaries. The variation of S ions with the value of ϕ increasing looks like the result given by Stolterfoht *et al.*,[3−6] namely, the variation of angular distribution of Ne^{7+} with tilt angle. When the ϕ is relatively large ($\phi > 3°$), the count of T ions is very small but the count of S is large. With the value of ϕ decreasing, the counts of T ions and S ions both increase slowly. When the tilt angle ϕ is less than 2°, the count rate of T ions increases quickly. The two peaks will be superposed into one peak located near 0°. Not only does the count of the transmitted ions but also the centre of observation angle θ change with tilt angle ϕ. But the observation angle θ is less than ϕ.



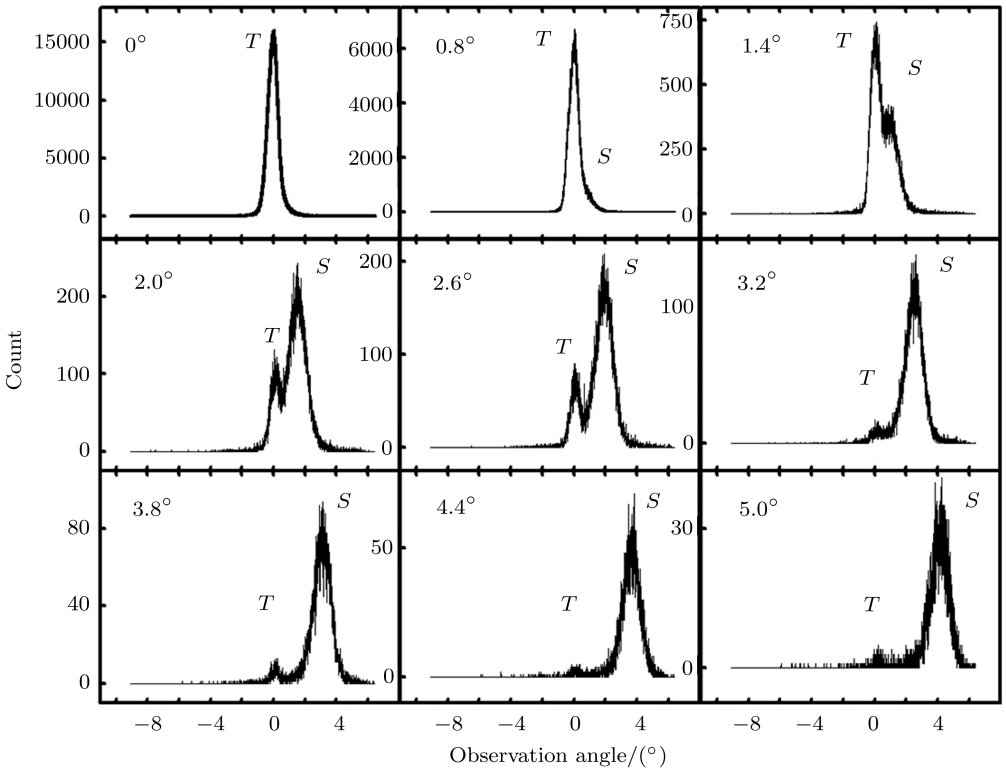


Fig. 2. Angular distributions of 18 keV Cl ions transmitted through Al_2O_3 nanocapillary foil without charge state analysis. The horizontal axis represents observation angle and vertical axis denotes count of transmitted ions. The figure on the top-left corner in each panel refers to tilt angle.

Figure 3 shows that the charge state distributions of transmitted ions are also different from those in the previous work. In Fig. 3 there occur four peaks: Cl_T^-, Cl_S^-, Cl_S^0, Cl_S^+ which belong to three charge states. The first peak that is located at $-3°$ is of negative ions Cl_T^-. Other three peaks are of negative ions Cl_S^-, neutral ions Cl_S^0 and positive ions Cl_S^+ scattered from the inner wall of the capillaries respectively, they all shift with the change of ϕ. The change of count of Cl_T^- ions is similar to that of the T ions. Count of Cl_S^0 is higher than those of Cl_S^- and Cl_S^+, and also larger than that of Cl_T^- at large ϕ but smaller than that of Cl_S^+ at small ϕ. There is one point that must be noticed that we cannot see Cl_S^+ at large ϕ. This is because the Cl_S^+ is out of detectible field. We believe that the T ions are comprised of ions Cl_T^- and that the S ions are composed of ions Cl_S^-, ions Cl_S^0 and ions Cl_S^+.

Figure 4 shows the transmission profile full widths at half maximum (FWHMs) of T ions, S ions, Cl_T^- ions, Cl_S^0 ions and Cl_S^+ ions. It clearly shows that the transmission profile FWHMs of T ions and Cl_T^- ions are nearly steady within the experiment uncertainties ($< 0.2°$). For S ions, the transmission profile FWHMs of Cl_S^0 ions and Cl_S^+ ions are very small ($1.1° <$ FWMH $< 1.7°$). The transmission profile FWHM of T ions is closest to that of Cl_T^- ions, the transmission profile FWHM of S ions is in the same range as those of Cl_S^0 ions and Cl_S^+ ions. But there exists a distribution for ions that have experienced an electrostatic analysis, but not for ions that do not have suffered an electrostatic analysis. This distribution may be caused by the electrostatic field. Figure 4 also shows that transmission profile FWHMs of S ions, Cl_S^0 ions and Cl_S^+ ions increase slimly with tilt angle ϕ decreasing within the experiment uncertainties($< 0.2°$). The transmission profile FWHM of Cl_S^+ ions is broader than that of Cl_S^0, which is possibly due to the larger energy range caused by their interactions with inner wall of capillaries.

Figure 5 shows the variations of angular distribution centres of T ions, S ions, Cl_T^- ions, Cl_S^- ions, Cl_S^0 ions and Cl_S^+ ions with tilt angle ϕ. Centres of angular distribution positions of S ions, Cl_S^- ions, Cl_S^0 ions and Cl_S^+ ions vary linearly with the value of ϕ. We can see that lines of S ions, Cl_S^- ions, Cl_S^0 ions and Cl_S^+ ions are parallel with each other. We define $\Delta\theta = \phi - \theta$. Figure 5 shows that $\Delta\theta$ increases with tilt angle ϕ increasing.

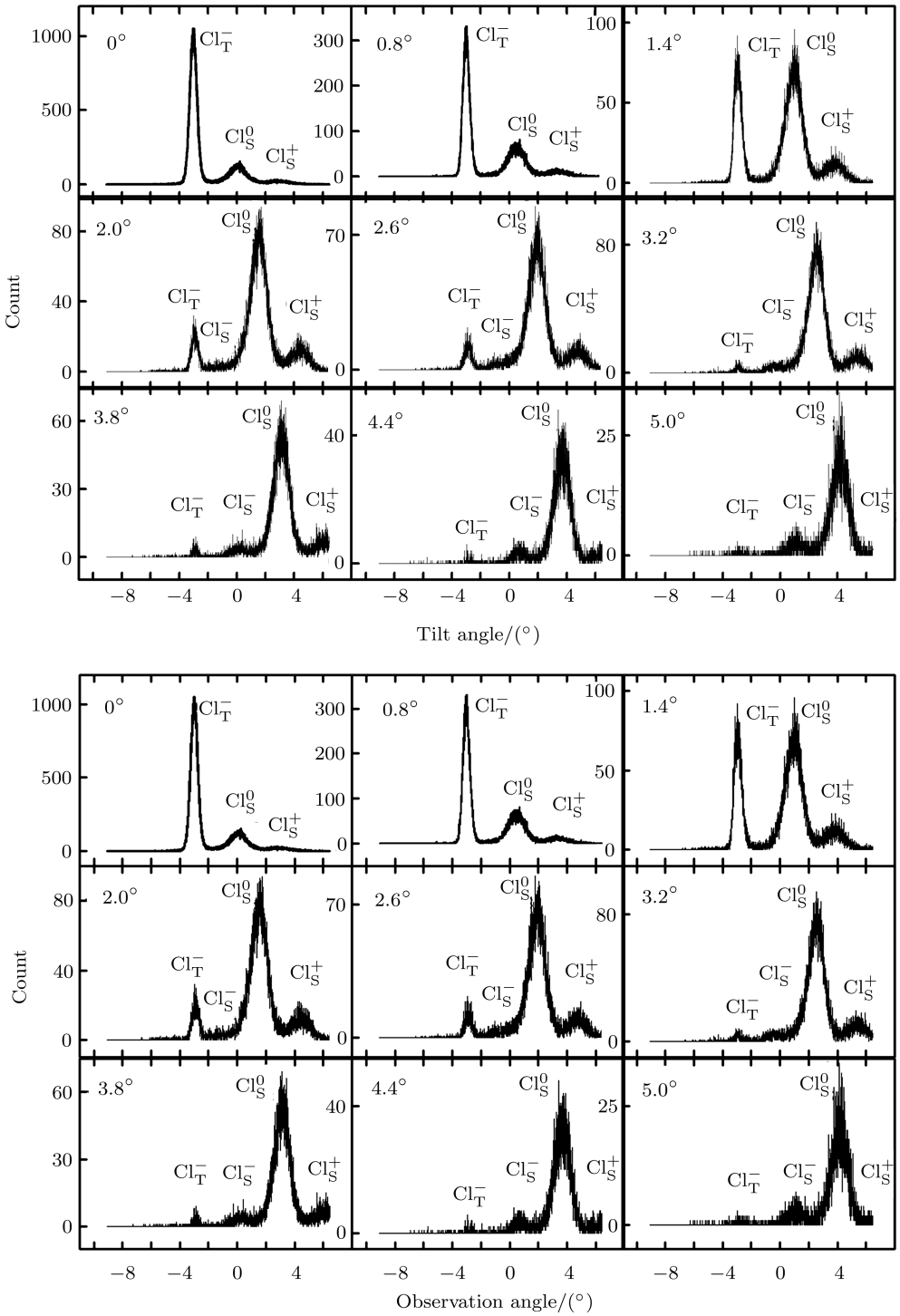


Fig. 3. Charge state distributions of 18 keV Cl ions transmitted through Al_2O_3 nanocapillary foil analysed by parallel-plate electrostatic analyzer. The horizontal axis represents observation angle and vertical axis denotes the count of transmitted ions. The figure on the top-left in each panel refers to tilt angle.

Considering the previous investigation of the angular distribution of the ions passing through the nanocapillaries, the value of $\Delta\theta$ should be equal to 0°. According to the second explanation for guiding effect we described earlier, Skog *et al.*[15] have established a model which is different from that given by Stolterfoht *et al.* In this model there were only a few charge patches formed sequentially in charge-up process. Inspired by their results, we establish a dynamic process (shown in Fig. 6) similar to theirs.

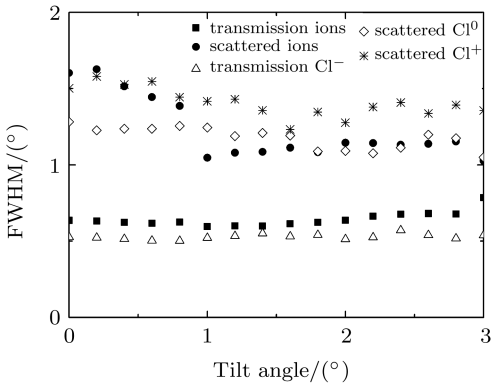


Fig. 4. Transmission profile widths (FWHMs) of T ions, S ions, Cl_T^- ions, Cl_S^0 ions and Cl_S^+ ions versus tilt angle for 18 keV negative Cl ions. The tilt angle varies from $\phi = 0$ to 3 in steps of 0.2°.

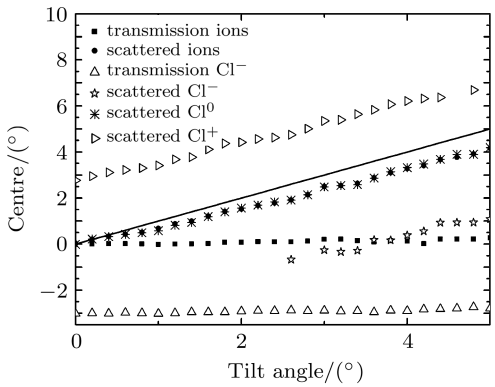


Fig. 5. Variations of angular distribution centres of T ions, S ions, Cl_T^- ions, Cl_S^- ions, Cl_S^0 ions and Cl_S^+ ions with tilt angle ϕ. Solid line represents the case where observation angle θ of transmitted ions is equal to tilt angle ϕ.

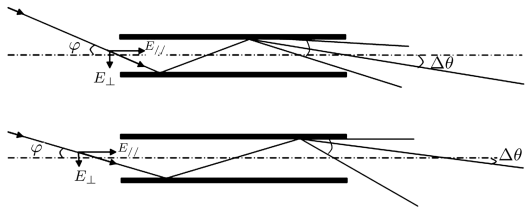


Fig. 6. Schematic diagram of dynamic progress of S ions transmitted from a capillary. $E_{//}$ and $E_\perp$ represent the horizontal and the vertical components of the kinetic energy of ions. The upper diagram represents larger tilt angle ϕ than the lower one.

Compared with high charge ions (HCIs), ionization energy of outermost electron of negative ions is more less than that of HCIs. Thereby negative ions will lose the outermost electrons easily during the collision with oxide surface,[17,18] and some of these ions are neutralized or ionized into positive ions further. Thereby the collision process is inelastic one, the charge exchange process and the slight energy loss cannot be avoided, so a slight energy loss happens besides the collision process. The energy lose comes mainly from vertical component of kinetic energy of incident ions.

We can see from Fig. 6 that after the first interaction of incident ions with the inner wall of capillary, the vertical component of kinetic energy of incident ions will be smaller than that before collision. It is easy to understand that trajectories of ions will approach the axis of the capillary. The second process is similar to the first one. After the second process trajectories of ions becomes nearly parallel to the axis of capillaries, there still exists a $\Delta\theta$ between trajectories of ions and axis of capillary. It is easy to see that when the tilt angle ϕ is increased, $\Delta\theta$ will also be increased. Owing to only two collision processes that are considered here, most of vertical component of kinetic energy of incident ions will be lost after the first collision process and then the trajectory will be highly approach the axis of capillary. On the other hand, if there exist three collision processes, θ will be larger than ϕ, it is discrepant with our experimental result.

On the other hand, our concern is the exit angle width scattered ions versus the opening angle of the last collision point to exit. It is clear that when the distance between the last collision point and the exit decreases, the opening angle increases, and then the exit angle width of scattered ions also increases. From Fig. 6 we can see that the opening angle increases with the decrease of the tilt angle ϕ. We can make a judgement that the exit angle half-width of scattered ions will increase with the decrease of the tilt angle ϕ, the conclusion is confirmed by experimental result.

In conclusion, we have measured the angular distribution of 18keV negative ions Cl^- which transmit through nanocapillaries in Al_2O_3 membrane with an aspect ratio of 200. Because of the ionization energy of negative ions is very small, the mechanism of negative ions transmitting through nanocapillaries is different from that of HCIs which have a strong ability to retain their charge state when transmitting through nanocapillaries. Most of the negative Cl^- ions will lose their outermost electrons after their first collision with the inner walls of the capillaries, and a slight energy loss caused by the inelastic collision process cannot be avoided. For this cause, the angular distribution centre and the angular distribution width of scattered ions varies with tilt angle. The mechanism of T ions transmitting through a nanocapillary is still an open

question: maybe it comes from the elastic collision of Cl^- ions with inner wall of capillary or it is caused by the poor collimation of capillaries. Timing effect of charge up process is not obtained only because a weak incident beam current is used. We will focus our attention on time effect and energy effect in our next work.

References

[1] Yamazaki Y 2002 *Nucl. Instr. and Meth Phys. Res.* B **193** 516

[2] Ninomiya S, Yamazaki Y, Koike F, Masuda H, Komaki K, Kuroki and Sekiguchi M 1997 *Phys. Rev. Lett.* **78** 4557

[3] Stolterfoht N, Bremer J H, Hoffmann V, Hellhammer R, Fink D, Petrov A and Sulik B 2002 *Phys. Rev. Lett.* **88** 133201

[4] Stolterfoht N, Hoffmann V, Hellhammer R, Pešic Z D, Fink D, Petrov A and Sulik B 2003 *Nucl. Instr. and Meth Phys. Res.* B **203** 246

[5] Stolterfoht N, Hellhammer R, Pešic Z D, Hoffmann V, Bundesmann J, Petrov A, Fink D and Sulik B 2004 *Vacuum* **73** 31

[6] Stolterfoht N, Hellhammer R, Sobocinski P, Pešic Z D, Bundesmann J, Sulik B, Shah M. B, Dunn K, Pedregosa J and McCullough R W 2005 *Nucl. Instr. and Meth Phys. Res.* B **235** 460

[7] Víkor G, Rajendra Kumar R T, Pešic Z.D, Stolterfoht N and Schuch R 2005 *Nucl. Instr. and Meth Phys. Res.* B **233** 218

[8] Sahana M B, Skog P, Víkor G, Rajendra Kumar R T and Schuch R 2006 *Phys. Rev.* A **73** 040901(R)

[9] Krause H F, Vane C R and Meyer F W 2007 *Phys. Rev.* A **75** 042901

[10] Chen Y F, Chen X M, Lou F J, Xu J Z, Shao J X, Sun G Z, Wang J, Xi F Y, Yin Y Z, Wang X A, Xu J K, Cui Y and Ding B W 2010 *Acta Phys. Sin.* **59** 0222 (in Chinese)

[11] Hellhammer R, Bundesmann J, Fink D and Stolterfoht N 2007 *Nucl. Instr Meth Phys. Res.* B **258** 159

[12] Hellhammer R, Sobocinski P, Pešic Z D, Bundesmann J, Fink D, Stolterfoht N 2005 *Nucl. Instr. and Meth Phys. Res.* B **232** 235

[13] Schiessl K, Palfinger W, Tökési K, Nowotny H, Lemell C and Burgdörfer J 2005 *Phys. Rev.* A **72** 062902

[14] Schiessl K, Palfinger W, Lemell C and Burgdörfer J 2005 *Nucl. Instr. and Meth Phys. Res.* B **232** 228

[15] Skog P, Zhang H Q and Schuch R 2008 *Phys. Rev. Lett.* **101** 223202

[16] Sun G z, Chen X M, Wang J, Chen Y F, Xu J K, Zhou C L, Shao J X, Cui Y, Ding B W, Yin Y Z, Wang X A, Lou F J, Lv X Y, Qiu X Y, Jia J J, Chen L, Xi F Y, Chen Z C, Li L T and Liu Z Y 2009 *Phys. Res.* A **79** 052902

[17] Winter H, Auth C, Hecht T and Mertens A 1999 *Nucl. Instr. and Meth Phys. Res.* B **157** 32

[18] Ustaze S, Verucchi R, Lacombe S, Guillemot L and Esaulov V A 1997 *Phys. Rev. Lett.* **79** 18